Nucleation of recrystallization

Ferdinand Knipschildt, Elisabeth Filippa

Published in:
Materials Science and Technology

Link to article, DOI:
10.1080/02670836.2022.2065054

Publication date:
2022

Document Version
Peer reviewed version

MATERIALS SCIENCE LITERATURE REVIEW PRIZE 2022

Nucleation of Recrystallization

Elisabeth Filippa Ferdinand Knipschildt[a]

[a] Technical University of Denmark, Department of Mechanical Engineering

ARTICLE HISTORY
Compiled April 29, 2022

ABSTRACT
Nucleation of recrystallization in deformed metals is discussed with focus on how theories have been achieved from experimental investigations. Suggested nucleation mechanisms and potential nucleation sites are reviewed to gain an overall understanding of the state-of-the-art. Limitations in the applied experimental techniques are discussed followed by an analysis of how newly invented non-destructive 3D techniques have challenged accepted theories which are based on 2D studies. Finally, suggestions for further studies by the novel and improved techniques are presented.

KEYWORDS
recrystallization; nucleation; metals; stored energy; 3DXRD; thermomechanical processing; nucleation site; nucleation mechanism

1. Introduction

Recrystallization is a crucial element of metal thermomechanical processing and is often used to control the properties and performances of the final products[1, 2]. During thermomechanical processing, the metal is typically deformed and during simultaneous or subsequent annealing, the microstructure evolves by recovery, recrystallization and grain growth[1, 3, 4], see Figure 1. Recovery, recrystallization and grain growth can in practice happen concurrently or sequentially[4]. These processes may happen during deformation (typically for hot deformation) or during annealing after cold deformation. During plastic deformation, the original grains change shape, the crystal lattices rotate towards preferred orientations and the number of dislocations and other defects increase by several orders of magnitude[5]. The dislocations are found to organise into cells (with less defects) surrounded by cell boundaries[6]. On a larger scale the microstructure is subdivided by dense dislocation walls and geometrically necessary boundaries (GNB) forming cell-block structures[7], see Figure 1. This results in an increase in stored energy in the form of excess dislocation/defect density[1, 5, 7]. The stored energy is a fraction of the energy supplied by the external load during deformation; the rest is released as heat[7, 8]. The driving force for recrystallization is generally described as the driving pressure[1, 9–11]:

$$F_r = \alpha G b^2 \rho \tag{1}$$

CONTACT Elisabeth Filippa Ferdinand Knipschildt. Email: effkn@mek.dtu.dk

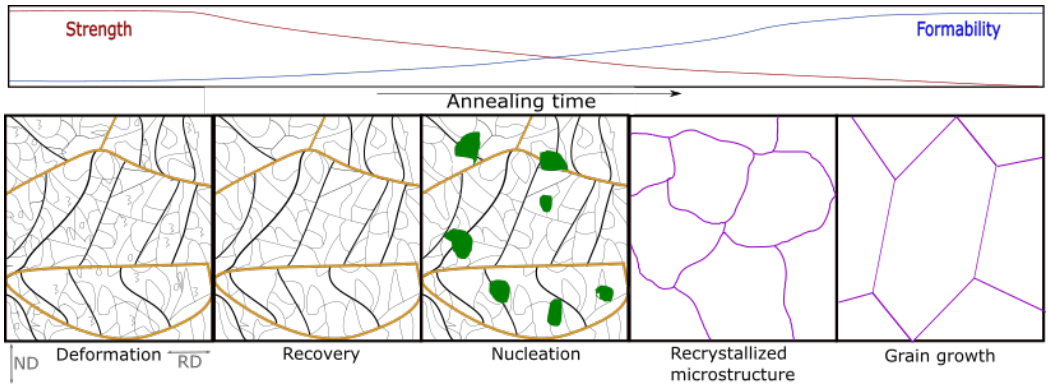

Figure 1. A very idealized and simple schematic diagram of the microstructure evolution and the change in mechanical properties during annealing. From left to right: the deformed state, the recovered state, nucleation, the fully recrystallized state and the microstructure after some grain growth. In the deformed, recovered and nucleation states the orange lines are the original grain boundaries, the thick black lines are GNBs and the thin black lines are cell boundaries. The recovered state illustrate partial defect annihilation and rearrangements. The green areas in the nucleation state are representations of nuclei. The purple boundaries in the recrystallized microstructure and that after some grain growth are newly formed grain boundaries. Figure adapted from reference[3] while the cell structure is inspired by reference[7].

where α is a constant (typically in the order of 0.5), G is the shear modulus, b is the Burgers vector and ρ is the dislocation density[1, 5, 12]. The local stored energy can be estimated experimentally by investigating the lattice distortion by synchrotron X-ray diffraction with suitable spatial resolution or electron microscopy, while measuring the heat released from the deformed sample during annealing using calorimetry gives the global stored energy[3, 8, 13]. It is worth noticing that the plastic deformation is rarely homogeneous[5] and the resulting stored energy then varies locally.

When annealing progresses, the processes after the deformation lower the stored energy[1], while the ordering increases[4], see Figure 1. During recovery, the density of dislocations and other defects decreases as these are annihilated and rearranged forming sub-grain boundaries[3, 14]. The sub-grain formation is also called polygonization[1, 3, 14, 15] and the sub-grain boundaries typically differ from grain boundaries by having smaller lattice misorientations[1]. The metal can recrystallize after deformation and/or recovery by forming nuclei with almost strain- and defect-free crystal lattices[1, 14]. Recovery lowers the stored energy thereby retarding the recrystallization process[16]. Nucleation of recrystallization can happen at different sites in the deformed microstructure[1, 14, 17], as illustrated in Figure 1. For recrystallization nucleation to take place, the decrease in stored energy of the deformed material, associated with introducing the almost defect-free nuclei, must theoretically be larger than the energy accompanying the increase in grain boundary area confining the nuclei[15]. However, areas of high stored energy do not necessarily lead to nucleation of recrystallization[9, 18, 19]. After the nuclei have obtained their critical sizes[20], the boundaries will migrate and the microstructure eventually becomes entirely replaced by the recrystallized microstructure. Grain growth may happen via boundary migration upon further annealing driven by boundary curvature and minimisation of the grain boundary inter-facial energies[1, 4]. The grain boundary mobility determines the migration velocity and is dependent on the grain boundary misorientation[1, 14, 21] as well as several other characteristics including grain boundary plane normal and annealing temperature[1]. High-angle grain boundaries have a much higher mobility than low-angle grain boundaries[1, 14, 21], thus being important for growth. High-angle grain

boundaries are defined as having misorientations larger than $10 - 15°$[5, 14, 22, 23].
The focus of this review is on nucleation of static recrystallization i.e. recrystallization *after* deformation. Recrystallization is in short defined as the creation of a new grain structure in a deformed material through the formation and migration of high-angle grain boundaries driven by the stored energy of deformation[22]. Recrystallization is often divided into the formation of new almost defect-free nuclei (i.e. nucleation) and the growth of these[1, 2, 7, 14, 20, 24]. Nucleation is a critical factor in determining both the size and crystallographic orientation of the resulting recrystallization microstructure and texture[21, 25, 26]. Thus, the mechanisms and parameters influencing the nucleation are of utmost importance[1, 27, 28]. Nucleation can be defined as a mechanism where dislocations rearrange in a deformed or recovered structure to create low dislocation density regions which have at least one high-angle grain boundary segment and thereby have the potential to grow relatively fast at the expense of the deformed matrix[1, 5]. Recrystallization nucleation may not be seen as a direct nucleation of new grains as in crystallization of for example water. This is because nucleation of recrystallization has been proposed to happen by either moving pre-existing high-angle grain boundaries or by creating new high-angle grain boundaries, meaning that the embryos of the nuclei are present in the deformed matrix[1]. For an embryo to become a nucleus it needs to grow into the deformed structure[29]. Yet, active nuclei may stop growing if they become surrounded by other active nuclei growing faster while some potential embryo might never start growing, because they are 'consumed' by other nuclei which have nucleated earlier. To differentiate between potential nuclei and active nuclei in-situ experiments are needed to follow their possible growth over time.
The nuclei sizes are small and they are few in number[1, 14, 17, 30]. The size of the critical nuclei depends on deformation strain[1], however they are often found experimentally in the order of ~ 1 μm. Experimental studies of nucleation have thus been referred to as looking for a 'needle in a haystack'[17]. Another obstacle for studying the nucleation sites, is when a recrystallized nucleus is formed, it replaces the deformed parent matrix, complicating the quantification of the matrix before the nucleation event. This is referred to as the 'lost evidence' problem[2, 4, 17, 30–33]. Yet, effective nucleation mechanisms and typical nucleation sites have been extensively studied, see Figure 2.
Detailed knowledge about nucleation is crucial when making models[17] to predict the recrystallized grain size and texture of the processed metal. Today, most models of nucleation are assuming that nucleation events are spread homogeneously through the microstructure[34] and have absolutely random orientations or orientations chosen within the spread of those present in the deformed state[13, 35]. This is mainly due to the lack of knowledge on how, where and why nucleation happens at the observed sites[13] and with which orientations, leaving many questions about nucleation yet to be answered[36].
In spite of the experimental challenges, several nucleation mechanisms have been suggested in the literature: the dominating ones in single-phase metals are strain-induced boundary migration (SIBM)[37], sub-grain coarsening and sub-grain coalescence[26], which will be reviewed in the following. For metals containing large second phase particles, particle stimulated nucleation (PSN) is suggested to be a dominating nucleation mechanism[12, 38–41], which likewise will be described in this review. Typical nucleation sites, which are generally agreed upon in literature for pure and more industrially relevant metals, include original grain boundaries[37], triple junctions[1], shear[42] and transition bands[43]. Here, nucleation is found to readily take place,

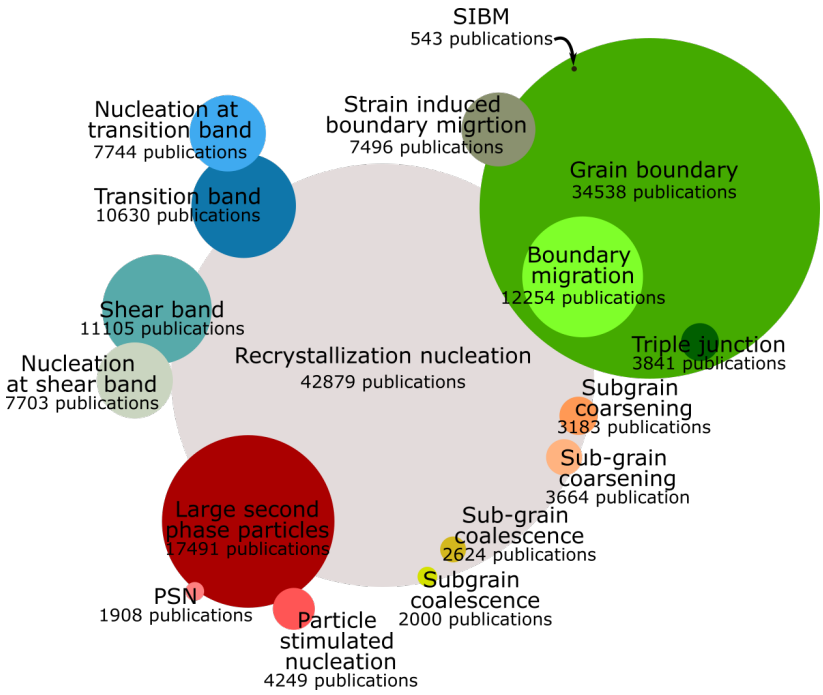

Figure 2. The number of publications found here: https://app.dimensions.ai/discover/publication. Only publications within the field 'material engineering' were included and the keywords: 'metal', 'recrystallization' and 'nucleation' were used in all searches. The numbers of publications were acquired November 2021.

however the exact position of the nucleation events at these preferred sites can not be predicted yet[1, 17, 30, 31]. These sites will be illustrated by literature examples in the following. Finally, a discussion of experimental limitations and new experimental possibilities, which will be biased towards 3D/4D experiments, is presented, leading to an outlook discussing how nucleation of recrystallization can be studied in the future and which essential questions regarding nucleation that should be addressed.

2. Nucleation mechanisms

Three nucleation mechanisms are mainly proposed for single-phase metals while PSN is of critical importance in particle-containing alloys. These are summarised in Figure 3 and will be reviewed in the following.

2.1. Strain induced boundary migration (SIBM)

During SIBM, a pre-existing high-angle grain boundary migrates into neighbouring grains creating small strain-free regions[17, 37], see schematics in Figure 3a. The migration of high-angle boundaries is induced by the strain build-up on each side of the boundary during deformation[5, 20]. For this mechanism to take place, the strain differences between the adjacent deformed grains must be large[5]. When the boundary moves, the stored energy will decrease as the defects and dislocations are eliminated[37], while the high-angle grain boundary surface area increases[5]. The nuclei formed by SIBM have similar orientations as those in the deformed materials from which they originate[1, 37]. Thus, if SIBM is dominating recrystallization, the texture

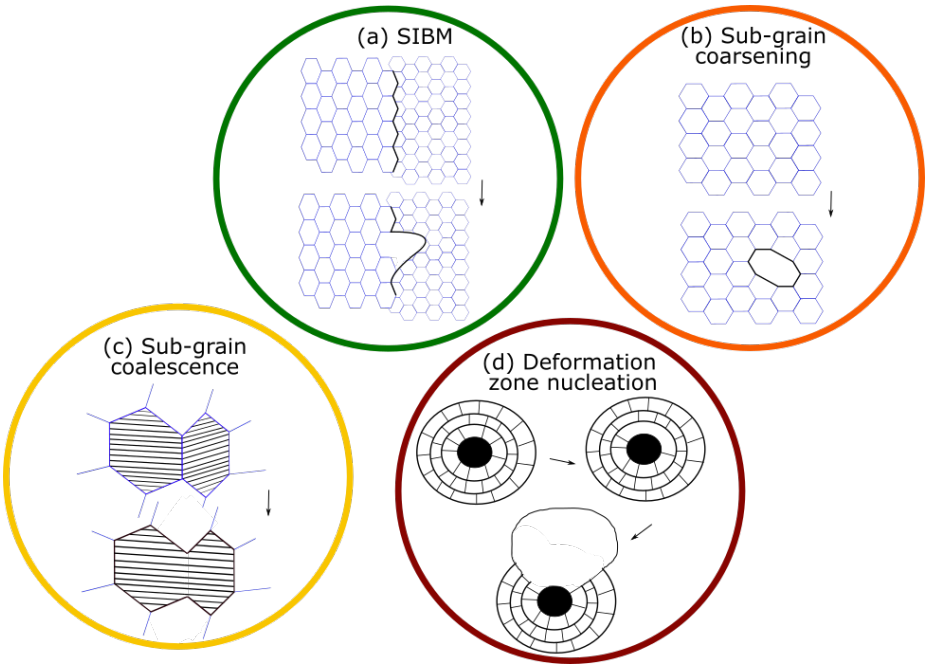

Figure 3. Schematics of the four nucleation mechanisms reviewed here. **(a)** strain induced boundary migration, **(b)** sub-grain coarsening, **(c)** sub-grain coalescence and **(d)** nucleation with a deformation zone surrounding a large second phase particle (shown in black). Figure inspired by references[5, 38]

will be closely related to the deformation texture[1], although the recrystallized texture will not be identical to the deformation texture as the nuclei select low stored energy orientations[44].

2.2. Sub-grain coarsening

Sub-grain coarsening is thermally assisted migration of low-angle boundaries at the expense of neighbouring sub-grains[5], see schematics in Figure 3b. The mechanism is driven by minimisation of stored energy as dislocations are eliminated and relocated. As the nucleus absorbs dislocations, the orientation difference relative to the matrix of the surrounding sub-grains increases, creating high-angle grain boundaries. The mechanism of coarsening can be seen as abnormal grain growth in a polygonized structure[1], where some sub-grains grow faster and then transform into nuclei. Sub-grain coarsening is thus expected to result in nuclei with orientations as those present in the deformed matrix[25].

2.3. Sub-grain coalescence

Coalescence occurs if two neighbouring sub-grains rotate, aligning their crystal lattices with respect to each other[26]. This results in the elimination of sub-boundaries and the formation of a larger sub-grain[5], as schematically shown in Figure 3c. Coalescence will change the orientation differences between the sub-grain and the adjacent matrix, leading to the formation of a somewhat higher angle boundary[5]. For the mechanism to happen it must be energetically favourable for the sub-grains to rotate in a direction which eliminate low-angle boundaries and create higher angle boundaries

towards the rest of the matrix[26]. However, it is debated whether this mechanism is a recrystallization mechanism and whether it plays a role in recrystallization[1, 20, 22], while some list coalescence as a recovery mechanism[14]. Coalescence of sub-grains is found to mostly happen in transition bands or regions next to grain boundaries i.e. in regions having a large distribution of sub-grain orientations[5, 43, 45].

3. Nucleation sites

Typical nucleation sites in both single-phase metals and metals containing large second phase particles are reviewed in the following supported by experimental results reported in literature.

3.1. Grain boundaries and triple junctions

Large orientation gradients have been found near grain boundaries[46–48]. This is expected to be a result of large strain gradients across the grain boundaries, which is due to the different selection of active slip systems in the two grains on either side of the grain boundary[1]. The larger stored energy, due to the large buildup of defects, at such grain boundaries is expected to explain nucleation at these sites[1]. The accumulation of lattice misorientations may be even larger at triple junctions, making triple junctions powerful nucleation sites[20, 40]. However, whether nucleation at grain boundaries and triple junctions is always an effect of SIBM, as described in section 2.1, is not clear[1].

Figure 4 shows an example of nucleation near a triple junction in 30% cold-rolled aluminium after annealing. The data was obtained using electron backscatter diffraction (EBSD)[17]. A nucleus, marked $A01$, has grown by SIBM during annealing from an original grain boundary close to a triple junction with an orientation highly related to the orientation of the parent grain. The largest misorientation between the parent and the nucleus found for this type of nucleation in this particular study was $< 10^\circ$, which was assumed to be within the spread of orientations in the parent grain. The nucleus seen in Figure 4b is not a perfect crystal; it contains low-angle boundaries which are illustrated by white lines. A slight variance of orientations within the nucleus arising from nucleation at grain boundaries has also been observed elsewhere[37]. The top part of Figure 4b is another nucleus, yet it is not known where it originated from and it is thereby not discussed in any detail in the paper[17].

An example of nuclei at an original grain boundary with orientations not directly related to the parent grains is shown in Figure 5. Here, nuclei labelled B01 and B02 have orientations not found in the deformed state[17]. In the study, one third of the recorded 29 nuclei showed new orientations with possible orientation relations to the deformed matrix being between $20^\circ - 55^\circ$ around one of four principal axes, $\langle 111 \rangle$, $\langle 112 \rangle$, $\langle 100 \rangle$ and $\langle 110 \rangle$[17]. New orientations were, in this study, defined as orientations not found in the deformed state; with a misorientation of more than 10° to the closest orientation observed in the deformed matrix. Relations between new orientations and the parent matrix within this range were also found in reference[25] in a high-purity nickel sample using EBSD. Here, new orientations were defined as orientations that fall outside the spread of orientations of the deformation sample[25]. Furthermore, both Al−1%wtMn[49], Ni, Cu and Al−2%wtCu[50] samples showed orientation relations between nuclei of new orientations in the partly recrystallized state and the deformed matrix. This was also found using EBSD. Here, the angle rotation ranges

(a) Before annealing. (b) After annealing.

Figure 4. Maps of orientations obtained by EBSD showing nucleation near a triple junction in a 30% cold rolled high-purity aluminum sample annealed at temperatures between 588 and 593 K for $10-15$ minutes. The white lines indicate misorientations between $1^\circ - 10^\circ$and the black lines mis-orientations $> 10^\circ$. Figure from reference[17].

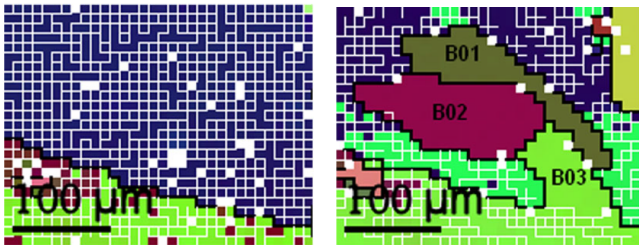

(a) Before annealing. (b) After annealing.

Figure 5. Maps of orientations obtained by EBSD showing multiple nuclei at an original grain boundary in a 30% cold rolled high-purity aluminum sample. The white lines indicate mis-orientations between $1^\circ - 10^\circ$and the black lines misorientations $> 10^\circ$. Figure from reference[17].

were observed to be slightly more narrow ($25^\circ - 55^\circ$) and the axes around which the nuclei with new orientation rotated were also somewhat different; $\langle 111\rangle$, $\langle 112\rangle$, $\langle 122\rangle$, $\langle 012\rangle$[49, 50] and $\langle 123\rangle$[50]. In reference[50], how new orientations are defined is not clearly stated, while in reference[49] orientations not coinciding with orientations observed in the deformed state are said to be new.
Neither of the mechanisms mentioned in section 2 can explain the formation of nuclei with new orientations[49]. It has been questioned if such nuclei could originate from sites below the surface[1, 2, 51], however this will be further discussed in section 5.

3.2. Nucleation at transition bands

Transition bands are regions of high lattice distortion in the deformed microstructure resulting from inhomogeneous deformation[52]. During plastic deformation, a grain can split, as a consequence of slip processes, into regions of different orientations with a band between the regions[43, 45, 53, 54]. These bands are called transition bands and are ideal for nucleation as they have large orientation gradients[1, 20]. The top micrograph in Figure 6 shows sub-grains elongated horizontally in the transition band. From diffraction patterns misorientations across the transition band were found to be as large as 30° over just 3 μm[52]. The horizontal boundaries separating the elongated sub-grains are transition band boundaries and mainly composed of geometrically necessary dislocations (GNDs), while the boundaries perpendicular to these, seen in Figure 6 as dark areas vertically crossing the transition band boundaries, are random boundaries consisting of statistically stored dislocations[52].
Nucleation in transition bands has in particular been observed for samples deformed

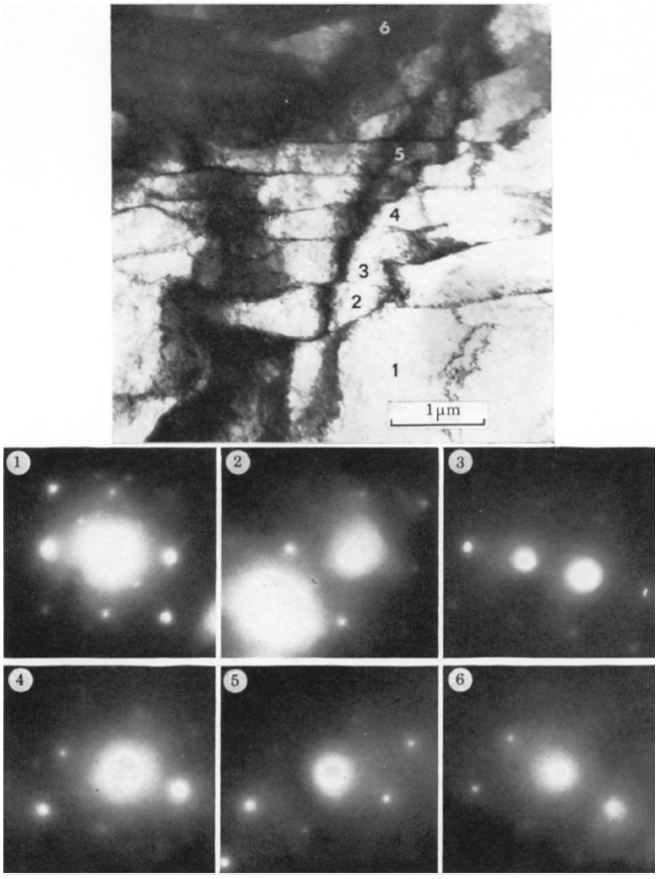

Figure 6. A horizontal transition band in a polycrystalline 50% cold rolled iron sample. The numbers of the different segments corresponds to each of the electron diffraction patterns. From reference[52].

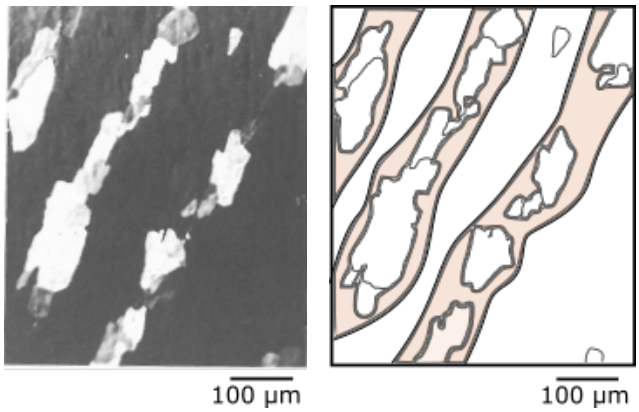

(a) (b)

Figure 7. Nucleation within microscopic shear bands in Al-Cu alloy. **(a)** An electron micrograph from reference[42] and **(b)** a new simple sketch highlighting the nuclei in **(a)**.

to high strains[41, 55] and the nuclei are observed to have orientations within the spread of the orientations within the transition band[41]. The orientations of the nuclei formed in transition bands can thus be very different from the ones in the neighbouring grains[43].
Nucleation of recrystallization in transition bands is well documented[45], however the mechanism is not clear: It has been suggested that nucleation at transition bands is due to the transition band boundaries migrate by SIBM on either side of the transition band forming nuclei which grow into the bands[55]. It has also been suggested that the nucleation happens by sub-grain coalescence due to the wide distribution of sub-grain orientations in transition bands[5].

3.3. Nucleation at shear bands

Shear bands can be either macroscopic or microscopic referring to their extent through the sample[14]. Macroscopic shear bands can cross through several grains and may expand across the thickness of the sample[44]. Whereas, microscopic shear bands are seen inside individual grains accommodating plastic strain[44]. The shear bands referred to in this section are macro shear bands and these are known to be preferable nucleation sites[14, 42].
Shear bands can arise in rolled metals as thin regions of highly strained material[56] often orientated $\sim 35^\circ$ to the rolling plane[1, 44]. Each shear band is accompanied by large shears[57]. The formation of these shear bands depends on deformation conditions, composition, texture and microstructure of the metal[1], however they especially develop in low stacking fault energy materials[27, 57]. Shear bands possess high stored energy and large orientation variations across the bands, which is assumed to be responsible for the high number of nucleation events observed here[14, 20]. An example of local recrystallization at shear bands in an Al-Cu alloy can be seen in Figure 7.
Recrystallized textures originating from nucleation within shear bands have no obvious correlation to the deformation texture[1] and nuclei with widely different orientations are found here[56]. The nucleation mechanism at these sites is not clarified[1].

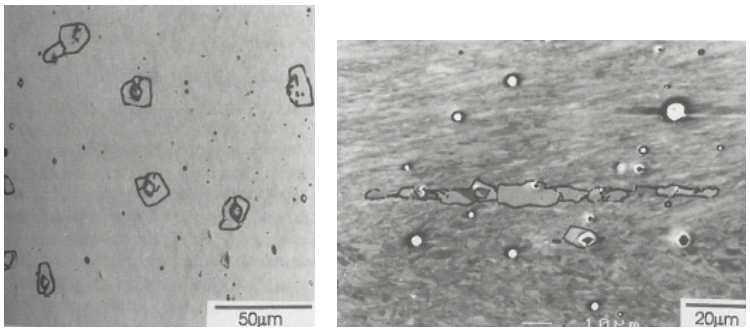

(a) $\epsilon = 0.5$ (b) $\epsilon = 2.3$

Figure 8. Backscattered electron micrographs from scanning electron microscopy (SEM) showing PSN at large SiO_2 particles in two Ni samples. **(a)** The sample was deformed to moderate strain ($\epsilon = 0.5$). **(b)** The sample was deformed to high strain ($\epsilon = 2.3$). Figures from reference[41].

3.4. Nucleation at large second phase particles

Second phase particles in metals are known to have great effects on recrystallization: large particles accelerate nucleation while small dispersoids retard boundary migration[58, 59]. Here, PSN at large second phase particles (> 1 μm in diameter)[12, 28, 38, 41, 42, 60] will be summarised.

During deformation, orientation gradients may be created by lattice rotations around large, hard second phase particles[20]. This is because dislocation slip is being hindered by the large second phase particles, forcing rotations in the matrix adjacent to the particles to reduce the lattice mismatches induced by deformation[28, 40]. The dislocations introduced are both GNDs and statistically stored dislocations, resulting in a very high dislocation density within the deformation zones[38]. A criterion for deformation zones to appear is that the deformation temperature is low, since at higher temperatures the dislocations can climb and escape the particle sites[12].

Recovery will eliminate many of the statistically stored dislocations and rearrange the GNDs into sub-boundaries[38], forming a deformation zone as seen in the first sketch in Figure 3d. Nucleation has been found to take place in these deformation zones by rapid sub-boundary migration replacing the deformation zone around the particle or a part of it[40]. This can be described as coarsening[38] and is shown schematically for a deformation zone in Figure 3d. The sub-grains in the deformation zones are relatively small and the local misorientations are high compared to the deformed matrix, meaning that the boundaries do only need to migrate a short distance before high-angle boundaries are formed compared with coarsening in a single-phase polygonized structure[38, 40]. The stored energy in the recovered deformation zone is also larger than in the matrix since the dislocation density is higher[38]. This results in a higher polygonization rate in deformation zones leading to accelerated nucleation here[38].

An example of PSN in Ni samples at large second phase SiO_2 particles can be seen in Figure 8. Here, the particles were estimated to be ~ 5 μm. In Figure 8a the sample was deformed to moderate strain ($\epsilon = 0.5$)[41] and recrystallization nuclei have developed at all large particles.

Due to the nature of deformation zones, the texture of metals recrystallized at large second phase particles is highly rotated[12, 28, 42, 60] as the orientations of the nuclei are inherited from the deformation zones[12, 61]. PSN has been shown to occur even more often at particles in grain boundaries, this has been assigned to the high local plastic strain here[46]. It has additionally been suggested to be due to the pre-exsting

high-angle boundaries at the particle sites which can readily migrate[41].
Several details on PSN are not known. It is for example not known how the particle size, particle shape, strain and neighbouring matrix orientations affect the nucleation behaviour nor why nucleation does not necessarily take place at every large second phase particle[41]. However, the dislocation density in the deformation zone is expected to affect the PSN behaviour. It is predicted to depend on strain (ε), particle volume fraction (F_v), particle size (r) and the dislocation Burgers vector (b)[12, 14]:

$$\rho_p = \frac{3\varepsilon F_v}{rb} \tag{2}$$

This equation shows the dislocation density is directly proportional to the strain. Furthermore, as the particle volume fraction is kept constant, the dislocation density will increase with decreasing particle radii.
When the Ni sample with large SiO_2 particles, shown in Figure 8, was deformed to higher strains, nucleation was solely observed at second phase particles in transition band[41], see Figure 8b. This illustrates how PSN is highly affected by strain[41], but also how PSN is not directly dependent on equation 2.
PSN is predicted to be an important mechanism, since nucleation near large second phase particles is found to dominate the recrystallization process in for example many aluminium alloys[39, 62]. The exact nucleation mechanism and why nucleation rarely takes places at all large second phase particles[41] are however not known.

4. Limitations in characterisation of recrystallization nucleation

The knowledge presented above on nucleation mechanisms and potential nucleation sites has been acquired through years of microscopy studies of recrystallization. A historical overview can be found in reference[5]. Yet, the suggested nucleation mechanisms can not explain why nuclei of new orientations have been observed in various cases as e.g. in Figure 5. In regard to new orientations, no general definition has been agreed on in terms of the orientation difference between the nuclei and parent grain. Additionally, it is not known why nucleation only sometimes takes place at some of the preferred nucleation sites[1, 17, 30, 31] but not at others even though the nucleation criteria are fulfilled there. This lack of knowledge is expected to be due to experimental limitations[4, 30].
The first criterion for successful investigations of nucleation is sufficient spatial resolution to reveal the nuclei i.e. sub-micron resolution[2]. Generally, laboratory X-ray diffraction and optical microscopy do not fulfil this criteria[20]. Yet, optical microscopy has been used for other important findings regarding nucleation, as e.g. in 1950 when Beck and Sperry[37] revealed the growth direction of SIBM. This was possible since the investigation of the growth does not require as high resolution as the initiation of nucleation does. The work of Gottstein from 1986[63] is an example of early use of a synchrotron source to investigate individual grains in a bulk polycrystalline Ni sample. In this early work, it was possible to determine the orientations of the grains and the nature of the boundaries separating them by Laue patterns[63]. However, the resolution was not good enough to be able to investigate nuclei.
Other experimental techniques provide high spatial resolution making it possible to easily reveal nuclei of recrystallization[24]. An example of the usage of SEM can be seen in Figure 8, here the partly recrystallized structure is imaged. Transmission elec-

tron microscopy (TEM) and high voltage TEM have been used to investigate the nucleation of thin samples[51, 64, 65]. TEM has furthermore been used to find the orientations of the nuclei and relate them to those in the deformed microstructure, e.g.[56]. This work must have been very time consuming and the orientations obtained are only from a small area in the sample making the observations of less general relevance. EBSD[66, 67] has been widely used to investigate nuclei orientations in recent years[7]. Compared to TEM, EBSD has the advantage of covering a much larger area, and although the spatial resolution is poorer it is still sufficient for nucleation studies. Even though the above-mentioned characterisation methods have sufficient resolution, they still possess two main obstacles. When only a thin surface layer is investigated, knowledge about the bulk of the sample is left out[24, 36], meaning that a grain observed on the surface of the sample can potentially be a result of nucleation happening at sites invisible to the researcher[33]. Furthermore, nucleation at the true sample surface is not necessarily representative for the bulk of the sample since surface effects, as e.g. scratches, might lead to odd nucleation behaviours[2, 30, 32, 68–70], potentially leading to wrong conclusions. Additionally, thin-film effects might influence TEM investigations[2]. There is thus a need for 3D measurement techniques. Static studies additionally lack information on what was present in the deformed matrix before the nuclei were formed[2] and they miss information on the nuclei being active or just potential. Humphreys did in 1977[38] acquire microscopy images recorded over time, showing the evolution of a nucleus formed by PSN. However, as these were surface observations, doubt exists if the result is representative for the bulk as well. There is thus a need for non-destructive high-resolution 3D techniques[2, 20] to investigate the nucleation events and to clarify the actual nucleation mechanisms observed at sites such as mentioned in section 3 along with other possible sites. In-situ 3D studies might eventually make it possible to predict at which sites nucleation will happen and with what orientation nuclei will form.

5. Recent 3D observations

Different suggestions of destructive 3D and non-destructive 3D nucleation investigations have been reported in literature[4, 24, 30–33, 36, 39, 62, 71–73]. Selected studies using different approaches of 3D and 4D (in-situ 3D) investigations will be reviewed in this section.

An example of a destructive 3D experiment is the study by Quey et al. in 2021[31]. Here, a columnar aluminium tricrystal was cold rolled to 40% thickness reduction along the columnar direction to create a sample microstructure which does not change significantly along this direction[31], see Figure 9a-b. This feature makes it possible to section the sample into slices along the rolling direction (RD) and then study these at different annealing stages, see Figure 9c. Slice number 5 was used to investigate the deformation structure and slice number 3 was used for analysing recrystallization[31]. By doing this the researchers could go 'back and forth in annealing time'. These slices were analysed by EBSD on the observation planes sketched in Figure 9d. It was found that recrystallization only occurred in crystal A and that the nuclei are closely related to the deformation structure[31]. Crystal A had the largest averaged stored energy among the three crystals, estimated from orientation maps acquired by EBSD[31]. Yet, within crystal A the highest density of nuclei was not found in the local region of highest stored energy, but in a region with large anisotropic orientation distributions[31]. This confirms, as stated in section 1, that the stored energy as the

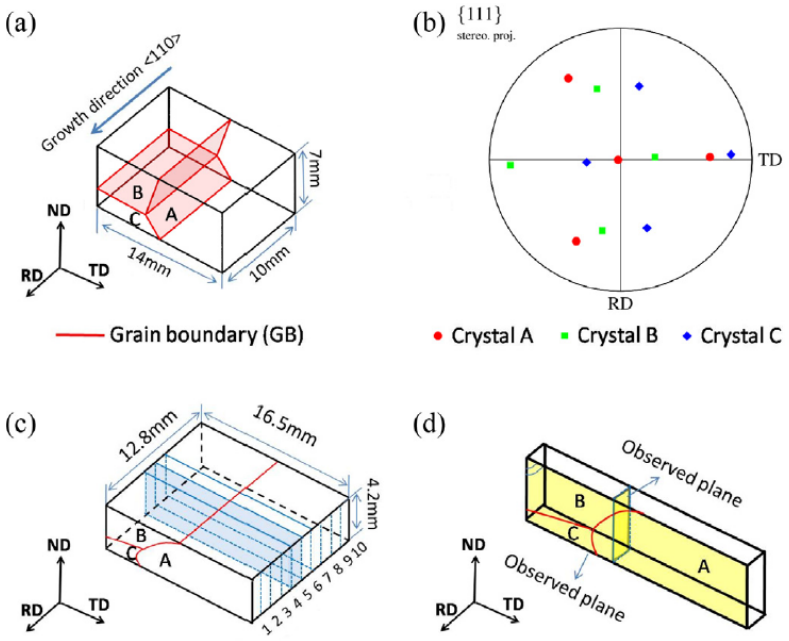

Figure 9. Schematics of high-purity aluminum tricrystal and how it is split into 10 slices. **(a)** The columnar microstructure of the initial sample. **(b)** The orientations of the three crystals labeled in a. **(c)** Shows the how the rolled sample was sliced into 10 smaller samples. Slide number 5 is shown in blue. **(d)** Shows the observation planes of the slices. From reference[31].

sole driving force for nucleation is an oversimplification. Thus, the authors derived a new primary stored energy expression including the anisotropy of the orientation distribution[31]. This type of experiment was carried out assuming the sliced samples were identical, yet this is not necessarily the case. Furthermore, the investigation might be subjected to surface effects as discussed in references[30, 32, 33]. This will not be further reviewed here but the primary stored energy would be an interesting theory to test in the future.

Another approach often seen in literature is EBSD combined with ion beam serial sectioning[7, 74]. Multiple parallel and closely spaced 2D sections are acquired by sectioning of the sample and doing EBSD on the newly created surface[75, 76]. This is then used to reconstruct the 3D sample volume[75–77]. However, besides surface effects[30, 32, 33] and surface damage due to ion bombardment[74], the ion sectioning might introduce misalignment between the different sections[75]. Furthermore, this method has not been used much for nucleation studies[76].

The mentioned sample sectioning techniques are, due to their destructive nature, unsuited for dynamic in-situ studies[73] of e.g. how nucleation of a specific nucleus takes place in the parent matrix. For this purpose three dimensional X-ray diffraction (3DXRD) using X-rays from synchrotron sources is much more suitable, exploiting the possibility of multiple non-destructive investigations of the same sample volume at different annealing stages. Several papers have been published[30, 32, 33]. The first 3DXRD measurement was in collaboration between Risø and European Synchrotron Radiation Facility[73]. A few examples, illustrating how important non-destructive 3D investigations are for studies of nucleation, will be reviewed in the following.

Nuclei of new orientations were suggested based on 2D EBSD[17], see e.g. Figure 5. However, it could not be ruled out that the nuclei did not originate from sites with

alike orientations below the surface. The possible formation of nuclei with new orientations is an important point in investigating the influence of the nucleation process on the final texture since 'odd nuclei' with orientations different from the matrix would have excellent growth potentials thus such nuclei could potentially lead to significant texture changes during recrystallization[32]. In the 3DXRD study by West et al.[33], 44 nuclei of new orientations were found on the surface, while 6 nuclei of new orientations were found in the bulk of the sample. The high amount of new orientations at the surface was attributed to surface scratches, which is a typical observation, e.g.[30, 33]. The six interesting nuclei of new orientation in the bulk of the sample were all found at triple junctions or grain boundaries[33]. In this study new orientations were defined as orientations different from any orientation with volume elements larger than 1 μm in the deformed parent grains[33]. The nuclei were all rotated around the same axes as found in reference[17], substantiating the observation of nuclei of new orientations in the paper based on just 2D observations.
As another example, the 3DXRD work by Larsen et al.[32] one nucleus, found in a triple junction, in a high-purity copper sample was also shown to have an orientation which was not within the spread of the deformed sample nor twin related[32].
How authors define nuclei of new orientations can vary and is likely to be affected by the resolution of the particular experimental method, as spatial and angular resolution can differ greatly, e.g. between EBSD and 3DXRD.
In general, twins are not included when referring to new orientations even though the orientations of the twins are not found in the parent matrix[1]. The twinning mechanism is well known[17] and not of high interest in regards to how non-twin-related new orientations form.
Whereas the above-mentioned 3DXRD nucleation studies focused on orientation relations, the microstructural evolution was followed in another non-destructive 3D study. Three ex-situ annealing steps, from recovery to recrystallization to grain growth, were investigated using near field high-energy X-ray diffraction microscopy (nf-HEDM) of a deformed high-purity aluminium sample[4]. The crystallographic orientations were recorded by focusing the X-ray beam on the planar 2D sample cross-section with a spatial resolution of 5 μm. These maps were then extended to 3D by measuring 11 consecutive cross-sections with 20 μm spacing. In Figure 10 the same area in each of the different annealing stages (from left to right: recovery, recrystallization and grain growth) is shown. The studied area is from the middle of the sample[4] to avoid possible surface effects. The nucleus was found in a region of high defect density (see Figure 10d). The nuclei mainly grew within the high defect-density volumes and not into neighbouring grains. In Figure 10g-i, it can be seen that as the nucleus grew, the adjacent grains somehow obtained more similar orientations to the matrix[4].
The latest detailed and non-destructive 3D work, relating an annealed state to the deformed state, is the study by Xu et al.[30] Here, a weakly cold-rolled aluminium sample was subjected to a hardness indentation. Nucleation was investigated using non-destructive 3D X-ray Laue microdiffraction, also called differential aperture X-ray microscopy (DAXM), with a high spatial resolution of $1.5 \times 1.5 \times 1.5$ μm^3[30]. Data was acquired before and after controlled annealing and the 3D volumes were reconstructed, see Figure 11. Nucleation was stimulated by the hardness indentation. This was chosen to ensure that some nuclei would develop within the volume mapped before annealing. In Figure 11 it can be seen that this approach was successful and several nuclei were found to develop near the indentation tip[30]. Here, 12 nuclei of orientations similar to the deformed matrix were observed[30]. From the study it was concluded that the nuclei were formed in areas of high stored energy by strain-induced

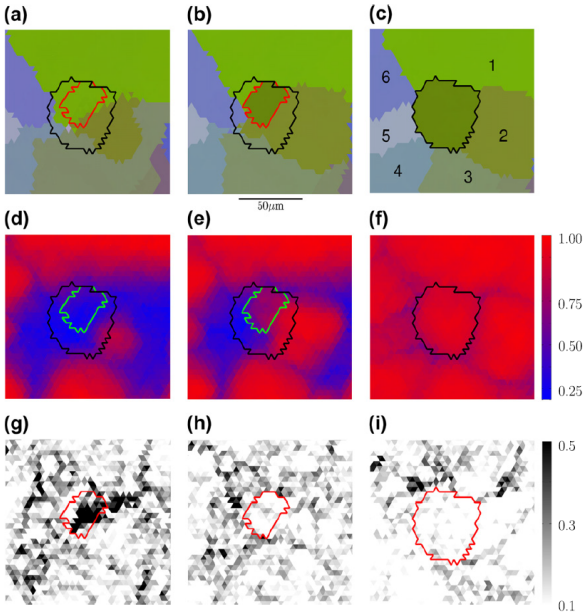

Figure 10. Measurements of a nucleation of a new grain during annealing of high-purity aluminum using nf-HEDM. From left to right the columns shows the initial, first and final state ie. the recovered site, the nucleated site and the site after some growth. **(a)-(c)** shows the orientations present in the 2D slice. **(d)-(f)** shows maps of the confidence metric, which is a measure showing where observed orientations match simulated ones. **(g)-(i)** Show misorientations between the nucleated grain and neighboring grains (obtained from kernel-averaged misorientation). From reference[4].

dislocation boundary migration[30], i.e. by a mechanism similar to SIBM but by migration of a different type of boundary than an original grain boundary.

3DXRD and DAXM in general provide excellent angular resolution[2]. A main limitation is the short time available for synchrotron experiments which typically means that only relatively small sample volumes can be mapped. Therefore, the nucleation experiments performed so far at synchrotron sources are experiments where the scientists have had some control of where nucleation would happen i.e. stimulated somewhat artificial nucleation situations. Additionally, the spatial resolution may be insufficient[2, 77] if samples subjected to high strains are investigated, as these can form very small nuclei[1]. Furthermore, the deformed micostructure can be difficult to investigate as plastically deformed grains give broadened diffraction patterns, making indexing problematic[33].

The high energy X-ray studies are constrained by synchrotron access limitations. However, laboratory X-rays techniques, as e.g. reference[39], would make 3D measurements more convenient and easier to access than synchrotron 3DXRD.

As something brand, new it was found that residual stress was present in recrystallized grains in a partially recrystallised Ni sample using DAXM[78]. This finding contradicts the assumption that recrystallization forms strain-free nuclei. It was furthermore observed that different recrystallized grains had unique elastic strain values[78]. If the existence of such variations of local elastic strains is found to be a general phenomenon, it is expected to be of utmost importance for the understanding of the recrystallization process.

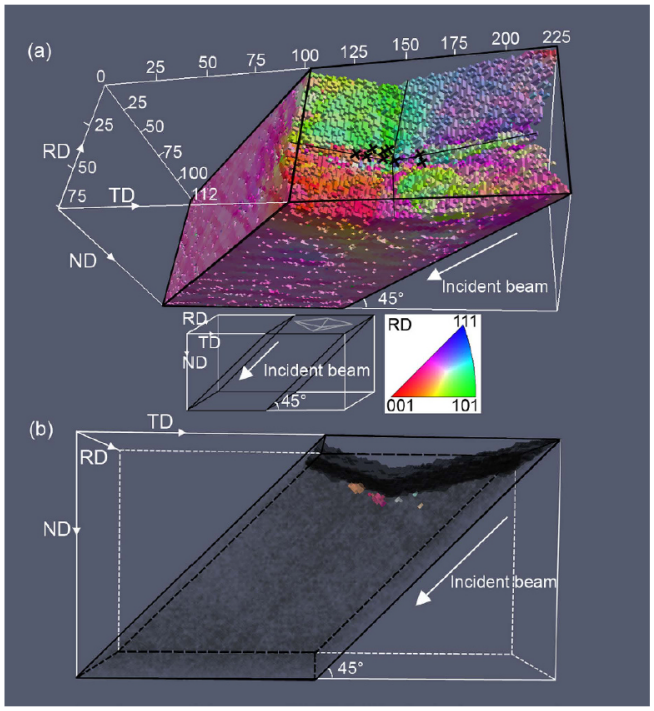

Figure 11. A selected volume of a cold rolled aluminum sample mapped in 3D by DAXM. **(a)** The spatial orientation distribution of the deformed sample near the indentation. **(b)** Side view of the embryonic volumes in the bulk sample near the indentation tip. The dark grey voxels are the indented surface and the light grey voxels are the total volume mapped. Figure from reference[30].

6. Summary

Nucleation of recrystallization in deformed metal with a primary interest in aluminium alloys has been reviewed. Well-documented nucleation mechanisms for single-phase metals as SIBM, sub-grain coarsening and sub-grain coalescence, along with PSN in metals containing large second phase particles, have been reviewed, while common nucleation sites have been illustrated by literature examples. Some focus was put into studies showing nuclei with new orientations, since this is an observation which can not be explained by the widely accepted nucleation mechanisms mentioned in this review. Furthermore, limitations in the experimental methods were pointed out along with some general criteria for successful nucleation investigations and some general obstacles in 2D measurements were mentioned. Additionally, the inability to predict the exact site of the nucleation events was attributed to the experimental limitations. More recent in-situ 3D observations were reviewed along with suggested limitations for each of these approaches.

7. Outlook

In the near future further non-destructive 3D studies of nucleation of recrystallization are needed. So far, all non-destructive 3D studies were found to be for highly idealised samples, e.g. nucleation by hardness indentation[30], or within small sample volumes[4]. Future non-destructive 3D studies, for example utilising 3DXRD, should be aimed at verifying the described nucleation mechanisms and potentially look for

additional mechanisms which may explain observations of nuclei with orientations not present in parent matrix.
In-situ 3D investigations are ideal to test more advanced nucleation theories. This could for example be the primary stored energy term suggested by Quey et al.[31] which includes the anisotropy of orientation distribution within the sample volume. As a result, the new methods might reveal additional parameters affecting the nucleation behaviour.
Besides 3D orientation measurements, future studies are suggested to include the effects of residual stress to possibly explain more thoroughly why nucleation takes place at some sites and not at others which are identical seen from a microstructural (orientational) perspective. Residual stress might be the missing link in all nucleation theories.
Metal 3D printing is becoming a theme of interest. Yet, the influence of the microstructures developing during printing, which are critically different from those after conventional manufacturing, on nucleation mechanisms is not known. It is for example not known whether voids in the microstructure can act as nucleation sites and how they will affect the growth of the nuclei. It is therefore suggested to combine studies of voids with 3D investigations during annealing to advance the understanding of post-print annealing of additively manufactured samples.
All together, the bigger goal of utilising the novel non-destructive 3D techniques for nucleation studies is to formulate improved nucleation models, that can predict where nucleation will take place, how many nuclei will form and the crystallographic orientations of these. Such models would allow a substantial improvement in tailoring thermomechanical processing of metals.

Acknowledgement(s)

I would like to thank Prof. Dorte Juul Jensen, Senior Researcher Yubin Zhang, Senior Researcher Tianbo Yu and Prof. Ida Westermann for guidance, very valuable comments on this manuscript and for tireless discussions also during late hours.

Disclosure statement

No potential conflict of interest was reported by the author.

Funding

The author thanks financial support by the European Research Council (ERC) under the European Union's Horizon 2020 research and innovation program (M4D - grant agreement No. 788567).

References

[1] Humphreys FJ, Hatherly M. Recrystallization and related annealing phenomena. Oxford: Pergamon Press; 1995.
[2] Juul Jensen D, Zhang YB. Impact of 3d/4d methods on the understanding of recrystallization. Curr Opin Solid State Mater Sci. 2020;24(2). GA no. 788567.

[3] Awan I, Khan A. Recovery, recrystallization, and grain-growth. J Chem Soc Pak. 2019 01;41:1–42.
[4] Hefferan CM, Lind J, Li SF, et al. Observation of recovery and recrystallization in high-purity aluminum measured with forward modeling analysis of high-energy diffraction microscopy. Acta Mater. 2012;60(10):4311–4318. Available from: https://www.sciencedirect.com/science/article/pii/S1359645412002765.
[5] Rios P, Siciliano F, Sandim H, et al. Nucleation and growth during recrystallization. Mater Res-Ibero-Am J Mater. 2005 09;8.
[6] Liu Q, Yao Z, Godfrey A, et al. Effect of particles on microstructural evolution during cold rolling of the aluminum alloy aa3104. J Alloys Compd. 2009;482(1):264–271. Available from: https://www.sciencedirect.com/science/article/pii/S0925838809006562.
[7] Hansen N, Juul Jensen D. Deformed metals – structure, recrystallisation and strength. Mater Sci Technol. 2011;27(8):1229–1240. Available from: https://doi.org/10.1179/1743284711Y.0000000046.
[8] Bacroix B, Castalnau O, Miroux A, et al. Relations between deformed grain orientations, stored energy and nucleation characteristic. Proc 21th Risø Int Symp. 2000;:1–14.
[9] Lee DN. The evolution of recrystallization textures from deformation textures. Scr metall mater. 1995;32(10):1689–1694. Available from: https://www.sciencedirect.com/science/article/pii/0956716X9500256U.
[10] Baczmański A, Wierzbanowski K, Benmarouane A, et al. Stored energy and recrystallization process. Mater sci forum. 2007 03;539-543:3335–3340.
[11] Szpunar JA, Narayanan R, Li H. Computer model of recrystallization texture in aluminum alloys. Mater Manuf Process. 2007;22(7-8):928–933. Available from: https://doi.org/10.1080/10426910701451820.
[12] Humphreys FJ, Juul Jensen D. Structure and texture evolution during the recrystallisation of particle containing materials. Proc 7th Risø Int Symp. 1986;:93–106.
[13] Hurley P, Humphreys FJ. Modelling the recrystallization of single-phase aluminium. Acta Mater. 2003 08;51:3779–3793.
[14] Verlinden B, Driver J, Samajdar I, et al. Thermo-mechanical processing of metallic materials. Oxford: Elsevier Science; 2007.
[15] Doherty RD. The deformed state and nucleation of recrystallization. Met Sci J. 1974; 8(1):132–142. Available from: https://doi.org/10.1179/msc.1974.8.1.132.
[16] Stüwe HP, Padilha AF, Siciliano F. Competition between recovery and recrystallization. Mater Sci Eng A. 2002;333(1):361–367. Available from: https://www.sciencedirect.com/science/article/pii/S0921509301018603.
[17] West S, Winther G, Juul Jensen D. Analysis of Orientation Relations Between Deformed Grains and Recrystallization Nuclei. Metall Mater Trans A Phys Metall Mater Sci. 2010; 42:1400–1408.
[18] Lee DN. Maximum energy release theory for recrystallization textures. Met Mater Int. 1996;2:121–131.
[19] Ashby MF. The influence of particles on boundary mobility. Proc 1th Risø Int Symp. 1980;:325–336.
[20] Humphreys JF. Nucleation in recrystallization. MSF. 2004;:467–470, 107–116.
[21] Porter DA, Easterlnig KE. Phase transformations in metals and alloys. Boca Raton: Taylor and Francis; 2009.
[22] Doherty RD, Hughes DA, Humphreys FJ, et al. Current issues in recrystallization: a review. Mater Sci Eng A. 1997;238(2):219–274. Available from: https://www.sciencedirect.com/science/article/pii/S0921509397004243.
[23] Jones MJ, Humphreys FJ. Interaction of recrystallization and precipitation: The effect of al3sc on the recrystallization behaviour of deformed aluminium. Acta Mater. 2003;51(8):2149–2159. Available from: https://www.sciencedirect.com/science/article/pii/S1359645403000028.
[24] Lauridsen EM, Poulsen HF, Nielsen SF, et al. Recrystallization kinetics of individual bulk grains in 90 % cold-rolled aluminium. Acta Mater. 2003;51(15):4423–4435. Available

from: https://www.sciencedirect.com/science/article/pii/S1359645403002787.
[25] Wu GL, Juul Jensen D. Orientations of recrystallization nuclei developed in columnar-grained ni at triple junctions and a high-angle grain boundary. Acta Mater. 2007;55(15):4955–4964. Available from: https://www.sciencedirect.com/science/article/pii/S1359645407003345.
[26] Li JCM. Possibility of subgrain rotation during recrystallization. J Appl Phys. 1962; 33(10):2958–2965. Available from: https://doi.org/10.1063/1.1728543.
[27] Driver JH, Paul H, Glez JC, et al. Relations between deformation substructure and nucleation in fcc crystals. Proc 21th Risø Int Symp. 2000;:35–48.
[28] Engler O, Kong XW, Yang P. Influence of particle stimulated nucleation on the recrystallization textures in cold deformed al-alloys part i—experimental observations. Scr Mater. 1997;37(11):1665–1674. Available from: https://www.sciencedirect.com/science/article/pii/S1359646297003151.
[29] Haasen P. Direct observation of nucleation and formation of the recrystallization texture in deformed single crystals of cu, al, cup. Proc 7th Risø Int Symp. 1986;:69–74.
[30] Xu C, Zhang YB, Godfrey AW, et al. Direct observation of nucleation in the bulk of an opaque sample. Sci Rep 7. 2017;42508.
[31] Quey R, Fan G, Zhang YB, et al. Importance of deformation-induced local orientation distributions for nucleation of recrystallisation. Acta Mater. 2021;210:116808. Available from: https://www.sciencedirect.com/science/article/pii/S1359645421001889.
[32] Larsen AW, Poulsen HF, Margulies L, et al. Nucleation of recrystallization observed in situ in the bulk of a deformed metal. Scr, Mater. 2005;53(5):553–557. Available from: https://www.sciencedirect.com/science/article/pii/S135964620500268X.
[33] West SS, Schmidt S, Sørensen HO, et al. Direct non-destructive observation of bulk nucleation in 30% deformed aluminum. Scr Mater. 2009;61(9):875–878. Available from: https://www.sciencedirect.com/science/article/pii/S1359646209004850.
[34] Vandermeer R, Rath B. Modeling recystallization kinetics in a deformed iron single crystal. Metall Mater Trans A. 1989;20(3):391–401.
[35] Rollett AD. Overview of modeling and simulation of recrystallization. Prog Mater Sci. 1997;42:79–99.
[36] Xu W, Quadir MZ, Ferry M. A high-resolution three-dimensional electron backscatter diffraction study of the nucleation of recrystallization in cold-rolled extra-low-carbon steel. Metall Mater Trans A Phys Metall Mater Sci. 2009;40(7):1547–1556.
[37] Beck PA, Sperry PR. Strain induced grain boundary migration in high purity aluminum. J Appl Phys. 1950;21(2):150–152. Available from: https://doi.org/10.1063/1.1699614.
[38] Humphreys FJ. The nucleation of recrystallization at second phase particles in deformed aluminium. Acta metall. 1977;25(11):1323–1344. Available from: https://www.sciencedirect.com/science/article/pii/0001616077901092.
[39] Lei X, Zhang YB, Sun J, et al. Particle stimulated nucleation revisited in three dimensions: a laboratory-based multimodal x-ray tomography investigation. Mater Res Lett. 2021; 9(1):65–70. Ga number: 788567 (M4D).
[40] Humphreys FJ. Recrystallization mechanisms in two-phase alloys. Met Sci J. 1979;13(3-4):136–145. Available from: https://doi.org/10.1179/msc.1979.13.3-4.136.
[41] Humphreys FJ, Ferry M, Johnson C, et al. Particle-stimulated nucleation - recent developments. Proc 16th Risø Int Symp. 1995;:87–104.
[42] Hirsch J, Engler O. Texture, local orientation and microstructure in industrial al-alloys. Proc 16th Risø Int Symp. 1995;:49–62.
[43] Hutchinson WB. Development of textures in recrystallization. Met Sci J. 1974;8(1):185–196. Available from: https://doi.org/10.1179/msc.1974.8.1.185.
[44] Kestens LAI, Pirgazi H. Texture formation in metal alloys with cubic crystal structures. Mat Science and Techn. 2016;32(13):1303–1315. Available from: https://doi.org/10.1080/02670836.2016.1231746.
[45] Dillamore IL, Katoh H. The mechanisms of recrystallization in cubic metals with particular reference to their orientation-dependence. Met sci. 1974;8(1):73–83. Available from:

https://doi.org/10.1179/msc.1974.8.1.73.
[46] Mishra SK, Pant P, Narasimhan K, et al. On the widths of orientation gradient zones adjacent to grain boundaries. Scr Mater. 2009;61(3):273–276. Available from: https://www.sciencedirect.com/science/article/pii/S1359646209002589.
[47] Barlow CYJ, Bay B, Hansen N. A comparative investigation of surface relief structures and dislocation microstructures in cold-rolled aluminium. Phil Mag A. 1985;51(2):253–275. Available from: https://doi.org/10.1080/01418610.1985.12069161.
[48] Randle V, Hansen N, Juul Jensen D. The deformation behaviour of grain boundary regions in polycrystalline aluminium. Phil Mag A. 1996;73(2):265–282. Available from: https://doi.org/10.1080/01418619608244382.
[49] Paul H, Miszczyk MM, Driver JH. Crystallographic aspects of nucleation and growth during primary recrystallization in stable single crystals of al and al-1%mn alloy. Proc 36th Risø Int Symp. 2015;:123–138.
[50] Miszczyk M, Paul H, Driver J, et al. New orientation formation and growth during primary recrystallization in stable single crystals of three face-centred cubic metals. Acta Mater. 2015;83:120–136. Available from: https://www.sciencedirect.com/science/article/pii/S1359645414007447.
[51] Haasen P. Recent results on the generation of new orientations during recrystallization. Czech J Phys B. 1988;38(4):354–358.
[52] Dillamore IL, Morris PL, Smith CJE, et al. Transition bands and recrystallization in metals. Proc R Soc Lond, A Math phys sci. 1972;329(1579):405–420. Available from: http://www.jstor.org/stable/78241.
[53] Hu H. Recovery and recrystallization of metals. Inter sci. 1962;:311–361.
[54] Nes E, Hutchinson WB. Texture and grain size control during processing of metals. Proc 10th Risø Int Symp. 1989;1:233–249.
[55] Bellier SP, Doherty RD. The structure of deformed aluminium and its recrystallization—investigations with transmission kossel diffraction. Acta Metall. 1977;25(5):521–538. Available from: https://www.sciencedirect.com/science/article/pii/0001616077901924.
[56] Ridha AA, Hutchinson WB. Recrystallisation mechanisms and the origin of cube texture in copper. Acta Metall. 1982;30(10):1929–1939. Available from: https://www.sciencedirect.com/science/article/pii/0001616082900335.
[57] Duggan BJ, Hatherly M, Hutchinson WB, et al. Deformation structures and textures in cold-rolled 70:30 brass. Met Sci. 1978;12(8):343–351. Available from: https://doi.org/10.1179/030634578790433909.
[58] Mandal D, Baker I. On the effect of fine second-phase particles on primary recrystallization as a function of strain. Acta Mater. 1997;45(2):453–461. Available from: https://www.sciencedirect.com/science/article/pii/S1359645496002157.
[59] Chan HM, Humphreys FJ. The recrystallisation of aluminium-silicon alloys containing a bimodal particle distribution. Acta Metall. 1984;32(2):235–243. Available from: https://www.sciencedirect.com/science/article/pii/000161608490052X.
[60] Chan HM, Humphreys FJ. Effect of particle stimulated nucleation on orientation of recrystallized grains. Met Sci J. 1984;18(11):527–530. Available from: https://doi.org/10.1179/030634584790419700.
[61] Juul Jensen D, Hansen N, Humphreys FJ. Texture development during recrystallization of aluminium containing large particles. Acta Metall. 1985;33(12):2155–2162. Available from: https://www.sciencedirect.com/science/article/pii/0001616085901762.
[62] Zhang Y, Juul Jensen D, Zhang YB, et al. Three-dimensional investigation of recrystallization nucleation in a particle-containing al alloy. Scr Mater. 2012;67(4):320–323. Available from: https://www.sciencedirect.com/science/article/pii/S1359646212003107.
[63] Gottstein G. Orientation determination in very small volumes using synchrotron radiation. Scr Mater. 1986;20(12):1791–1794. Available from: https://www.sciencedirect.com/science/article/pii/0036974886902905.
[64] Jones A, Ralph B, Hansen N. Subgrain coalescence and the nucleation of recrystallization of grain boundaries in aluminium. Proc Math Phys Eng. 1979;368(1734):345–357.

[65] Faivre P, Doherty RD. Nucleation of recrystallization in compressed aluminium: studies by electron microscopy and kikuchi diffraction. J Mater Sci. 1979;14:897–919.
[66] Dingley DJ, Longden M, Weinbren J, et al. On-line analysis of electron back scatter diffraction patterns. i. texture analysis of zone refined polysilicon. Scanning Microsc. 1987; 1(2):451–456). Available from: https://digitalcommons.usu.edu/microscopy/vol1/iss2/2.
[67] Krieger Lassen NC, Juul Jensen D, Conradsen K. Image processing procedures for analysis of electron back scattering patterns. Scanning Microsc. 1992;6(1). Available from: https://digitalcommons.usu.edu/microscopy/vol6/iss1/7.
[68] Beck PA, Sperry PR, Hu H. The orientation dependence of the rate of grain boundary migration. J Appl Phys. 1950;21(5):420–425. Available from: https://doi.org/10.1063/1.1699676.
[69] Fan G, Zhang Y, Driver J, et al. Oriented growth during recrystallization revisited in three dimensions. Scripta Materialia. 2014;72-73:9–12. Available from: https://www.sciencedirect.com/science/article/pii/S1359646213004971.
[70] Liebmann B, Lucke K, Masing G. Orientation dependency of the rate of growth during primary recrystallization of a1 single crystals. Z metallkd. 1956;47:57–63.
[71] Zhang YB, Budai J, Tischler J, et al. Boundary migration in a 3d deformed microstructure inside an opaque sample. Sci Rep. 2017 12;7.
[72] Pokharel R, Lind J, Li SF, et al. In-situ observation of bulk 3d grain evolution during plastic deformation in polycrystalline cu. Int J Plast. 2015;67:217–234. Available from: https://www.sciencedirect.com/science/article/pii/S0749641914002083.
[73] Fu X, Poulsen HF, Schmidt S, et al. Non-destructive mapping of grains in three dimensions. Scr Mater. 2003;49(11):1093–1096. Available from: https://www.sciencedirect.com/science/article/pii/S135964620300513X.
[74] Juul Jensen D, Poulsen H. The three dimensional x-ray diffraction technique. Mater Charact. 2012;72:1–7.
[75] Pirgazi H. On the alignment of 3d ebsd data collected by serial sectioning technique. Mater Charact. 2019;152:223–229. Available from: https://www.sciencedirect.com/science/article/pii/S1044580319306394.
[76] Xu W, Ferry M, Cairney JM, et al. Three-dimensional investigation of particle-stimulated nucleation in a nickel alloy. Acta Mater. 2007;55(15):5157–5167. Available from: https://www.sciencedirect.com/science/article/pii/S1359645407003680.
[77] Lin F, Godfrey A, Jensen DJ, et al. 3d ebsd characterization of deformation structures in commercial purity aluminum. Materials Characterization. 2010;61(11):1203–1210. Available from: https://www.sciencedirect.com/science/article/pii/S1044580310002457.
[78] Zhang YB, Barabash RI. High resolution mapping of orientation and strain gradients in metals by synchrotron 3d x-ray laue microdiffraction. Quantum Beam Sci. 2019;3(1). Available from: https://www.mdpi.com/2412-382X/3/1/6.